Analysis of Layered Ejecta Craters with Mars Reconnaissance Orbiter Shallow Radar (SHARAD) Data.

Z. M. Bain[1], N. E. Putzig[1], S. J. Robbins[2], R. H. Hoover[2,3] ,A. M. Bramson[4], E. I. Petersen[4], G. A. Morgan[1]. [1]Planetary Science Institute (1546 Cole Blvd #120, Lakewood, CO zbain@psi.edu), [2]Southwest Research Institute, [3]University of Colorado at Boulder, [4]Lunar and Planetary Laboratory, University of Arizona.

Introduction: Impact craters have been observed on nearly every planetary surface and can be used to understand surface geologic properties and composition. Craters with layered ejecta (LE) deposits make up nearly one-quarter of Martian craters and have been observed on several other planetary bodies [1]. There are two main hypotheses for the formation of LE craters. The volatile fluidization model assumes that an impactor is hitting a volatile-rich target, melting or vaporizing the subsurface volatiles [2]; the atmospheric entrainment model assumes ejecta material, the atmosphere, and vortices created during impact interact in such a way to create the LE appearance [3]. While the volatile fluidization model has had more support in the literature, there is no definitive study establishing which mechanism is predominant on Mars.

Hoover et al. [4] used thermophysical data derived from the Mars Odyssey Thermal Emission Imaging System (THEMIS) and Mars Global Surveyor Thermal Emission Spectrometer (TES) to evaluate grain-size distributions, model horizontal mixing and vertical layering, and identify materials present in the ejecta deposits. Fifty LE craters were analyzed globally, with some measures of grain-size distribution providing evidence for either or both theories, but no overwhelming evidence was found in support of one over the other.

Previous work on LE craters has examined the surface through visible imagery and the very shallow subsurface (<1-2 m) with thermophysical data. For this work, we examined LE crater using Mars Reconnaissance Orbiter Shallow Radar (SHARAD) sounder data. SHARAD has the potential to sense through the whole ejecta blanket and provide estimates of bulk composition in cases where the ejecta layer is sufficiently thick (> ~ 15 m) to be resolved.

Methods: SHARAD transmits a swept 25-to-15 MHz signal, giving a freespace vertical resolution of 15 m [5]. When the radar waves encounter a change in dielectric properties part of the signal is reflected back toward the spacecraft. The returned signal is recorded and typically displayed using 2D radar profiles "radargrams" with along-track distance on the horizontal axis and delay time on the vertical axis (the latter can be converted to depth with knowledge of the wave speed in the different media encountered). When interpreting radargrams, it is import to consider surface returns from off-nadir "clutter" that may interfere with or be mistaken for subsurface returns. To mitigate this problem, we compare all radargrams used in this study to simulations of surface returns for nadir and off-nadir sources. This step is particularly important when examining LE as the topography of the crater, surrounding terrain and the ejecta itself can generate significant amounts of clutter that can be easily confused with subsurface returns.

As a part of a separate project (Subsurface Water Ice Mapping (SWIM) on Mars; see Putzig et al., this conference), ~6000 radargrams were analyzed across the northern hemisphere (up to 60°N). This work provided an opportunity to also look at LE craters in this region since the radargrams crossing LE craters were already being analyzed. Members of the SWIM Team examined the craters from Hoover et al. [4] and LE craters with equivalent ejecta radii greater than 24 km from the Robins and Hynek [6] crater catalog that were within the SWIM study region.

Once we have identified a subsurface return, we can sometimes use the topographic relief of the ejecta relative to the surrounding plains to estimate the depth to the subsurface reflector (presumed to be at the base of the ejecta). With this estimated depth, we can calculate the real dielectric permittivity (ε') of the ejecta layer, which can be used to constrain the composition of that layer.

Preliminary Results: To date, we have examined 28 craters for subsurface reflectors. Of these craters, we found good evidence of a subsurface reflector for 3 craters, inconclusive results for 8 craters, and either no reflectors or indecipherable clutter for the remaining 17 craters. All but 3 of the craters had significant amounts of clutter, highlighting the importance of using clutter simulations when studying these features.

For one of the craters with a subsurface reflector, we were able to confidently estimate ε'. All of the 20 observations crossing the LE blanket showed the reflector. For 6 of those observations, the topography allowed us to estimate the depth to the reflector. We found an average ε' of 4.22 with values ranging from 3 to 6. This low value for the dielectric permittivity is consistent with the LE containing a mixture or layering of roughly equal proportions of water ice and regolith.

Continued Work: After completing initial LE mapping within the SWIM study region, we will examine the remaining craters studied by Hoover et al.

[4] and those with equivalent ejecta radii greater than 24 km that did not fall within the SWIM study region. Additional LE craters may be analyzed if there is reason believe they are more likely to have subsurface returns (e.g., LE with low surface roughness). For LE craters that lie near enough to the polar region, we will use preexisting 3D SHARAD volumes that encompass the polar regions [7] to look for subsurface returns associated with the ejecta.

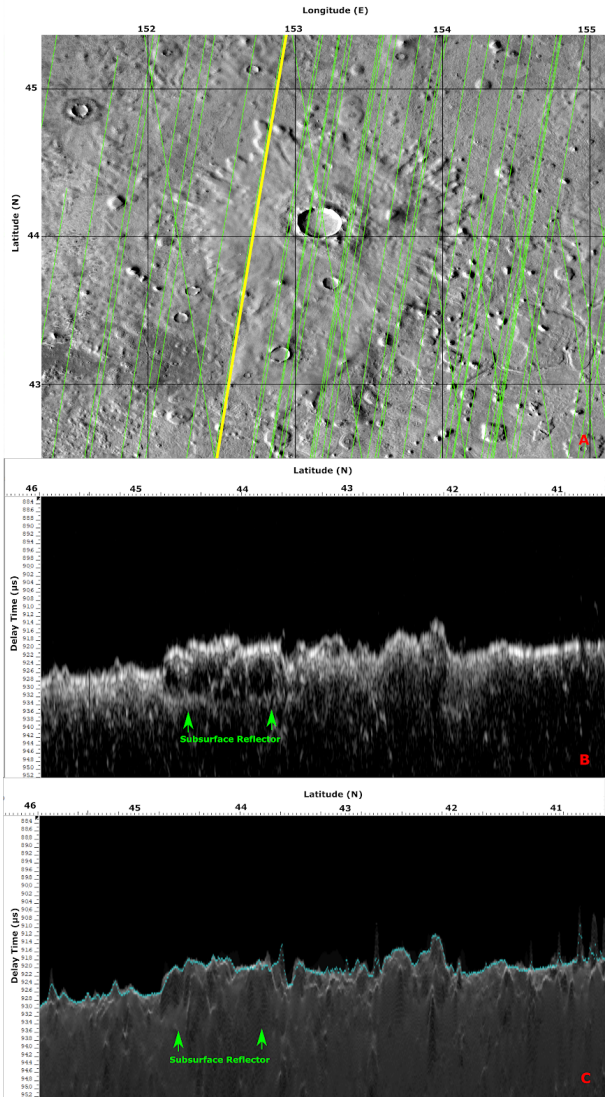

Figure 1. (a) Crater 07-00183 in THEMIS day IR with SHARAD coverage in green lines and observation 2355402 highlighted in yellow. (b) Radargram for SHARAD observation 23554-02 shows a strong apparent subsurface return (above green arrows) below the LE. (c) Clutter simulation for the same observation has no corresponding returns at the same delay time, supporting the interpretation of the reflector not being clutter.

As a final effort to derive information about LE craters with SHARAD, we will integrate techniques developed by Campbell et al. [8] and Bain et al. [9] to scrutinize the surface reflection seen by SHARAD. While SHARAD was designed to probe the subsurface through sounding, the surface reflection contains a wealth of information about surface roughness and near-surface Fresnel reflectivity. SHARAD surface returns can be used to give a measure of 10- to 100-m-scale roughness that is valuable in identifying craters with low clutter where subsurface reflections would be easier to identify[8].

Further work can be done to isolate the Fresnel reflectivity of the surface return, which provides a measure of the density of the shallow subsurface materials. Since ice is a low-density material, especially in comparison to the regolith and rock that make up most of Martian surface materials, measuring reflectivity offers a strategy to search for near-surface ice-rich deposits. Within this context, the 'surface return' is defined by the SHARAD central wavelength, which effectively samples the upper ~5 m of the subsurface. Consequently, the bulk density over this range can be constrained. As every SHARAD measurement includes a value of the surface power returned, we can generate density estimates across the planet and use them to search for regions of low power that can be indicative of shallow ice[9].

Conclusion: A better understanding of the formation process for LE craters on Mars can help us understand the geologic surface properties that were present during their formation. SHARAD is a powerful tool to help better understand the composition and density of these craters. Preliminary results show promise that we can use the radar data to better understand LE composition, but more work is needed to be able to make more definitive conclusions about LE craters based on SHARAD results.

References: [1]Barlow et al. (2000) JGR, 105, 26733-26738. [2] Carr et al. (1977) JGR, 82, 4055-4065. [3] Schultz and Gault (1979) JGR, 84, 7669-7687. [4] Hoover et al. (2019) JGR, Submitted,[5] Seu et al. (2007) JGR, 112. [6] Robins and Hynek (2012) JGR, 117 [7] Putzig et al. (2018) Icarus, 308, 138-147. [8] Campbell et al. (2013) JGR, 118, 436-450 [9] Bain et al. (2019) 50th LPSC Abstract #2726

Acknowledgments: This work is supported by NASA's Mars Data Analysis Program, award number NNX15AM48G. The SWIM project is supported by NASA through JPL Subcontract 1611855. We are grateful to SeisWare International Inc. for academic licensing of their Geophysics software used in our radar analysis.